

## Quantum interference effects in a system of two tunnel point-contacts in the presence of a single scatterer: simulation of a double-tip STM experiment

N. V. Khotkevych, Yu. A. Kolesnichenko, and J. M. van Ruitenbeek

Citation: *Low Temp. Phys.* **37**, 53 (2011); doi: 10.1063/1.3551531

View online: <http://dx.doi.org/10.1063/1.3551531>

View Table of Contents: <http://ltp.aip.org/resource/1/LTPHEG/v37/i1>

Published by the [American Institute of Physics](#).

---

### Related Articles

A Cartesian quasi-classical model to nonequilibrium quantum transport: The Anderson impurity model  
*J. Chem. Phys.* **138**, 104110 (2013)

High mobility half-metallicity in the (LaMnO<sub>3</sub>)<sub>2</sub>/(SrTiO<sub>3</sub>)<sub>8</sub> superlattice  
*Appl. Phys. Lett.* **102**, 042401 (2013)

Electron transfer through a single barrier inside a molecule: From strong to weak coupling  
*J. Chem. Phys.* **137**, 074110 (2012)

High-frequency gate manipulation of a bilayer graphene quantum dot  
*Appl. Phys. Lett.* **101**, 043107 (2012)

A single-electron probe for buried optically active quantum dot  
*AIP Advances* **2**, 032103 (2012)

---

### Additional information on *Low Temp. Phys.*

Journal Homepage: <http://ltp.aip.org/>

Journal Information: [http://ltp.aip.org/about/about\\_the\\_journal](http://ltp.aip.org/about/about_the_journal)

Top downloads: [http://ltp.aip.org/features/most\\_downloaded](http://ltp.aip.org/features/most_downloaded)

Information for Authors: <http://ltp.aip.org/authors>

### ADVERTISEMENT

**AIP**Advances

*Submit Now*

**Explore AIP's new  
open-access journal**

- **Article-level metrics  
now available**
- **Join the conversation!  
Rate & comment on articles**

## Quantum interference effects in a system of two tunnel point-contacts in the presence of a single scatterer: simulation of a double-tip STM experiment

N. V. Khotkevych and Yu. A. Kolesnichenko<sup>a)</sup>

*B. Verkin Institute of Low Temperature Physics and Engineering, National Academy of Sciences of Ukraine, 47 Lenin Ave., Kharkov 61103, Ukraine*

J. M. van Ruitenbeek

*Kamerlingh Onnes Laboratorium, Universiteit Leiden, Postbus 9504, Leiden 2300, The Netherlands*

(Submitted October 12, 2010)

Fiz. Nizk. Temp. **37**, 64–70 (January 2011)

The conductance of systems containing two tunnel point-contacts and a single subsurface scatterer is investigated theoretically. The problem is solved in the approximation of *s*-wave scattering giving analytical expressions for the wave functions and for the conductance of the system. Conductance oscillations resulting from the interference of electron waves passing through different contacts and their interference with the waves scattered by the defect are analyzed. The possibility of determining the depth of an impurity below the metal surface by using the dependence of the conductance on the distance between the contacts is discussed. It is shown that the application of an external magnetic field results in Aharonov-Bohm oscillations in the conductance, the period of which can be used to determine the depth of the defect in a double-tip STM experiment. © 2011 American Institute of Physics. [doi:10.1063/1.3551531]

With the development of scanning tunnelling microscopy (STM) it has become clear that a single STM probe is often not enough to obtain information on the detailed characteristics of the surface under investigation. A logical development of the one-tip approach is a dual-tip experimental setup, which can provide us with richer information than conventional single-probe STM. Despite the apparent technical complexity of the dual-tip STM (DSTM) in comparison with standard STM, several groups have successfully improved the STM technology in this way.<sup>1–4</sup>

DSTM can be realized in different ways. For example, it can be a spatially extended STM tip with two protrusions, each ending in a cluster or a single atom.<sup>5</sup> A second approach is a coaxial beetle-type double-tip STM design that seems advantageous in retaining the standard STM stability.<sup>6</sup> The most versatile DSTM employs two individual tips, which can be driven independently. In this case the distance between the tips is limited in principle only by a parameter such as the characteristic tip radius.<sup>2</sup> Another original example of DSTM is a proposal<sup>7</sup> in which one contact can be created directly on the surface, while the other is the STM tip itself.

For DSTM experiments with two independent probes there are different possibilities for applying voltages to the tunnelling contacts. There are two basic circuit designs: in the first, electrons are emitted from the first contact and then gathered at the second, i.e., the current flows from one contact to the other through the surface being probed.<sup>8,9</sup> This method can be used to obtain a trans-conductance map, and, in addition, permits implementation of three-terminal ballistic electron emission spectroscopy (BEES) without the introduction of macroscopically bounded contacts.<sup>3</sup> In the second basic scheme<sup>5</sup> a bias is applied between the two tips and the sample, i.e., the current flows from two contacts into the sample.

Subsurface defects, adatoms, and steps on a metal surface lead to the appearance of Friedel-like oscillations in the STM conductance  $G=dI/dV$ , i.e., a nonmonotonic variation in  $G$  with the distance between the STM tip and the defect  $r_0$ . (For a review see Ref. 10.) Studies of this variation can be used to detect buried defects and to investigate their characteristics. Methods for determining the positions of defects below a metal surface using a single tip STM have been proposed before: this can be achieved using the period of oscillations in the conductance as a function of bias<sup>11,12</sup> or by exploiting the interference pattern of the conductance as a function of position,  $G(r_0)$ , which is very pronounced in the open directions of the Fermi surface.<sup>13–15</sup> These approaches are very suitable for the surfaces of simple metals, such as the noble metals, but their application to conductors with more complicated Fermi surface geometries will be difficult and has not yet been explored.

Here we examine the simultaneous injection of electrons into the surface by the first and second contacts. We consider this realization of a double-tip experiment as a natural refinement of the single-tip STM problem for the study of single defects buried under a metal surface.<sup>11,12,15</sup>

The idea of using multiple tunnelling contacts for determining the depth and location of impurities under a metal or semiconductor surface has been discussed before.<sup>8</sup> The paper by Niu *et al.*,<sup>8</sup> proposes a method for determining the desired depth by measuring the transconductance between the two tips of a dual-tip scanning tunneling microscope. Here we propose a different approach: measuring the phase change  $\Delta\vartheta$  in the conductance oscillations as a function of the distance  $d$  between two STM tips. These phase changes can be measured experimentally with great precision. We show that  $\Delta\vartheta$  can be expressed in terms of the distance  $d$  (in units of the Fermi wave vector  $k_F$ ), the position  $\rho_0$  of the defect in a plane parallel to the surface, which is easily defined experi-

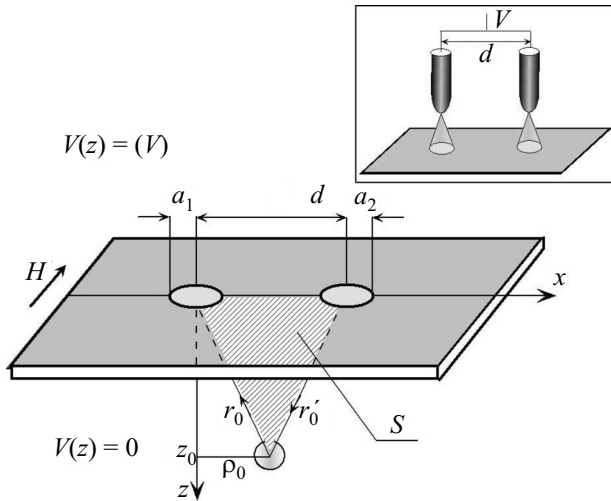


FIG. 1. Schematic arrangement of a system of two tunnel contacts, modelled as two orifices in an infinitely thin interface between conducting half-spaces. The inset shows the equivalent circuit with two STM tips, which provide electron tunnelling paths through small areas with characteristic radii  $a_1$  and  $a_2$ .

mentally, and the unknown depth of the defect,  $z_0$ . Thus, by measuring  $\Delta\vartheta(d)$  it is possible to determine the depth of a buried impurity. The procedure for determining  $z_0$  is further simplified when a magnetic field  $\mathbf{H}$  is applied to the system. Then the STM conductance  $G$  undergoes Aharonov–Bohm oscillations. These oscillations result from the quantization of the magnetic flux through the area formed by the electron trajectories from the contacts to the defect and the line connecting the contacts (Fig. 1). For a weak magnetic field the electron trajectories and the line connecting the contacts form a triangle, and the defect depth can be found easily from the area of the triangle,  $S$ .

As a model for the double-tip STM geometry we consider two metal half-spaces separated by an infinitely thin nonconducting interface at  $z=0$ , which contains two small regions (contacts) that allow electron tunnelling (see Fig. 1). The origin  $\mathbf{r}=0$  of the coordinate system is chosen to be in the center of the first contact. The  $x$ -axis is directed along the line connecting the contacts. For the potential barrier in the plane  $z=0$  we use the function<sup>17</sup>

$$U(\mathbf{r}) = U_0 f(\boldsymbol{\rho}) \delta(z). \quad (1)$$

In our case  $f(\boldsymbol{\rho})$  describes two «windows» for electron tunnelling and is reciprocal  $f^{-1}(\boldsymbol{\rho})$  can be written as a sum of two terms

$$f^{-1}(\boldsymbol{\rho}) = \chi(\rho/a_1) + \chi(|\mathbf{d} - \boldsymbol{\rho}|/a_2),$$

$$2\pi \int_0^\infty dx x \chi(x) = 1, \quad (2)$$

where  $\chi(x) \approx 1$  for  $x \leq 1$ , and  $\chi(x) \ll 1$  for  $x \gg 1$ ,  $a_{1,2}$  are the characteristic radii of the contacts,  $\rho$  is the component of the vector  $\mathbf{r}$  parallel to the plane  $z=0$ , and  $\mathbf{d}$  is a two-dimensional radius vector from the center of the first contact to the center of the second. The absolute value  $d$  is the distance between contacts, assuming that this is smaller than the shortest relaxation length.

A single defect described a short range potential  $D(\mathbf{r})$  is positioned in the vicinity of the contacts, with

$$D(\mathbf{r}) = g D_0(|\mathbf{r} - \mathbf{r}_0|), \quad (3)$$

where  $g$  is the interaction constant for the interaction of the electrons with the defect and  $D_0(|\mathbf{r} - \mathbf{r}_0|)$  is a spherically symmetric function localized within a region of characteristic radius  $r_D$  centered at the point  $\mathbf{r} = \mathbf{r}_0$ , which satisfies the normalization condition

$$4\pi \int_0^\infty dr' r'^2 D_0(r') = 1. \quad (4)$$

To calculate the conductance  $G$  we proceed as before. The probability density current is found by using the wave function  $\psi(\mathbf{r})$  for the electrons tunnelling through the potential barrier in the plane of the orifices. The total electric current  $I$  in the system is calculated by integrating over the electron momenta and over a surface that overlaps the contacts. We take the temperature to be zero, and assume a small applied voltage  $V$  consistent with the linear regime of Ohm's law,  $I = GV$ . Under these assumptions the conductance  $G$  can be written as

$$G = \frac{e^2 \hbar}{m^*} \nu(\varepsilon_F) \int_{S_F, v_z > 0} d\Omega_{\mathbf{p}} \int_S d\Omega r^2 \text{Im}[\psi^*(\mathbf{r}) \nabla \psi(\mathbf{r})]. \quad (5)$$

In Eq. (5)  $m^*$  is the effective electron mass,  $\nu(\varepsilon_F)$  is the electron density of states at the Fermi level, and  $d\Omega$  and  $d\Omega_{\mathbf{p}}$  are the elements of solid angle in geometric and momentum space, respectively. As the surface for spatial integration we choose a half-sphere of radius  $r$  greater than the distance between the contacts  $d$  and centered at the center of first contact,  $r=0$ , and covering the contacts in the lower half-space,  $z > 0$ . The integration with respect to the directions of the momentum over the Fermi surface  $S_F$  is carried out for electrons which tunnel and have a positive projection  $v_z$  of the electron velocity along the contact axis  $z$ . As a consequence of the conservation of the total current, the integral over  $d\Omega$  is independent of the length chosen for the radius  $r$ .

The electron wave function  $\psi(\mathbf{r})$  satisfies the Schrödinger equation

$$\left[ \nabla^2 + \frac{2m^*}{\hbar^2} (\varepsilon - D(\mathbf{r})) \right] \psi(\mathbf{r}) = 0, \quad (6)$$

subject to the boundary conditions of continuity and of the jump of its derivative at  $z=0$ . In Ref. 17 a solution of Eq. (6) has been found for an arbitrary function  $f(\boldsymbol{\rho})$  in the limit of weak tunnelling,  $1/U_0 \rightarrow 0$ , and for a purely ballistic contact (no defects present),

$$\psi_0(\boldsymbol{\rho}, z) = - \frac{ik_z \hbar^2}{(2\pi)^2 m^* U_0} \int_{-\infty}^{\infty} d\boldsymbol{\rho}' e^{i\boldsymbol{\rho}' \cdot \boldsymbol{\rho}} e^{ik_z' z} \int_{-\infty}^{\infty} d\boldsymbol{\rho}'' \frac{e^{i(\boldsymbol{\rho} - \boldsymbol{\rho}'') \cdot \boldsymbol{\rho}'}}{f(\boldsymbol{\rho}'')}, \quad (7)$$

where  $k_s' = \sqrt{\boldsymbol{\rho}^2 + k_z^2 - \boldsymbol{\rho}'^2}$ , and  $\kappa$  and  $k_z$  are the components of the vector  $\mathbf{k}$  parallel and perpendicular to the interface, respectively. As a special case the authors of Ref. 17 considered a system of several orifices with different radii.

The characteristic radius of the region through which the electrons tunnel from the STM tip into the sample has subatomic size ( $a \approx 0.1 \text{ \AA}$ ), while the Fermi wave vector is  $k_F \approx 1 \text{ \AA}^{-1}$ . By using the condition  $k_F a_{1,2} \ll 1$  we find, after integrating over  $\kappa'$  in Eq. (7),

$$\psi_0(\mathbf{r}) = \frac{it(k_z)}{2} \left[ (ka_1)^2 \frac{z}{r} h_1^{(1)}(kr) + (ka_2)^2 \frac{z}{r'} h_1^{(1)}(kr') e^{i\kappa d} \right] \quad (8)$$

where  $h_1^{(1)}(kr)$  is the spherical Bessel function of the first order,  $r' = |\mathbf{r} - \mathbf{d}|$ , and

$$t(k_z) = \frac{\hbar^2 k_z}{im^* U_0} \quad (9)$$

is the transmission amplitude of the electron wave function passing through a homogeneous barrier. Note that in the limit  $k_F a_{1,2} \rightarrow 0$  the result of Eq. (8) does not depend on the particular form of the function  $\chi(\rho/a)$  in Eq. (2), and the wave function Eq. (8), as well as the conductance of the system, are expressed in terms of the effective areas of the contacts,  $\pi a_{1,2}^2$ .

The effect of electron scattering by the short-range potential can be taken into account by the method proposed in Ref. 18. If the radius of action  $r_D$  of the potential  $D(\mathbf{r})$  is of the order of the Fermi wave length  $\lambda_F$ , then in the region of the defect  $|\mathbf{r} - \mathbf{r}_0| \lesssim r_D$  the wave function  $\psi(\mathbf{r})$  can be taken as a constant  $\psi(\mathbf{r}_0)$ . In this approximation, Eq. (6) becomes an inhomogeneous equation with its right-hand side equal to  $(2m^*/\hbar^2)D\psi(\mathbf{r}_0)$ . In the limit  $1/U_0 \rightarrow 0$  a solution of this equation can be expressed in terms of the solution of the homogeneous equation (see Eqs. (7) and (8)) and the retarded electron Green function of Eq. (6) for the semiinfinite half-space

$$\psi(\mathbf{r}) = \psi_0(\mathbf{r}) + \frac{2m^*}{\hbar^2} T(k) [G_0^{(+)}(|\mathbf{r} - \mathbf{r}_0|) - G_0^{(+)}(|\mathbf{r} - \tilde{\mathbf{r}}_0|)] \psi_0(\mathbf{r}_0), \quad (10)$$

where  $\tilde{\mathbf{r}}_0 = (\rho_0, -z_0)$ ,  $T(k)$  is the scattering matrix, which for a short-range scatterer can be expressed in terms of the s-wave scattering phase shift  $\delta_0$  as<sup>20</sup>

$$T(k) = \frac{-\pi \hbar^2 (e^{2i\delta_0} - 1)}{m^* ik \left( 1 + \frac{1}{4ikz_0} (e^{2i\delta_0} - 1) e^{2ikz_0} \right)}. \quad (11)$$

The Green function

$$G_0^{(+)}(x) = -\frac{\exp(ikx)}{4\pi x} \quad (12)$$

is the retarded Green function for a free electron. The phase shift  $\delta_0$  is given in terms of the scattering strength  $g$  by

$$e^{i\delta_0} \sin \delta_0 = -\frac{m^* kg}{2\pi \hbar^2} \left( 1 - \frac{8\pi m^* g}{\hbar^2} \int_0^\infty dr G_0^{(+)}(r) D(r) \right)^{-1}. \quad (13)$$

Figure 2 illustrates the spatial variation of the wave function (10) for the case when the contacts and the scatterer all lie in the  $y=0$  plane. The interference of electron waves

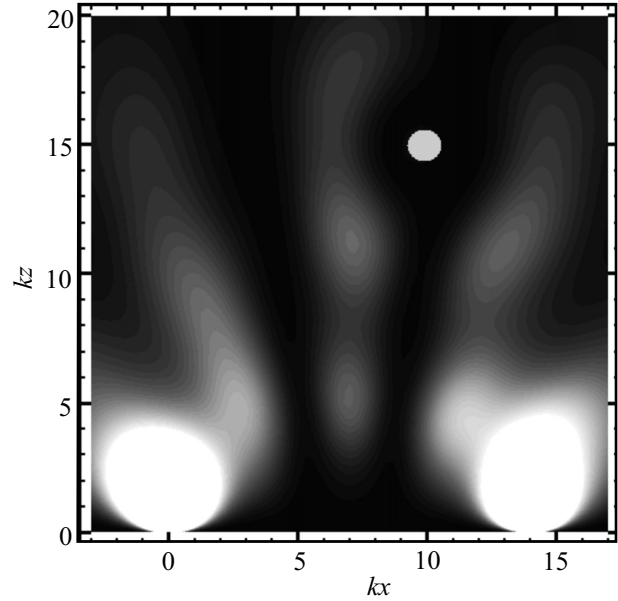


FIG. 2. Squared modulus of the wave function (10). The defect is located at  $kr_0 = (10, 0, 15)$ , the distance between the contacts  $kd = 14$ , and the scattering phase shift is  $\delta_0 = 1.5$ .

passing through different contacts and their interference with the waves scattered by the defect are clearly visible. In order to make the effects more visible, in Fig. 2 we have used a large value for the scattering phase,  $\delta_0 = 1.5$ , which is acceptable only for Kondo resonance scattering by a magnetic impurity (see, for example,<sup>19</sup>). The grey circle round the point  $\mathbf{r} = \mathbf{r}_0$  in Fig. 2 is the region in which the Eq. (10) is not valid because the Green function diverges.

Substituting the wave function (10) into the general expression (5) for the conductance  $G$  we find

$$G = G_c(a_1, a_2) + G_{\text{osc}}, \quad (14)$$

where  $G_c$  is the conductance of the double contact system in the absence of the defect

$$G_c(a_1, a_2) = G_0(a_1) + G_0(a_2) + G_{12}, \quad (15)$$

$G_0$  is the inherent conductance of a single contact<sup>17</sup>

$$G_0(a) = |t(k_F)|^2 \frac{e^{2(k_F a)^4}}{36\pi \hbar}, \quad (16)$$

and  $G_{12}$  takes the interference of electron waves passing through different contacts into account,

$$G_{12} = |t(k_F)|^2 \frac{e^{2(k_F a_1)^2} (k_F a_2)^2}{18\pi \hbar} f^2(k_F d). \quad (17)$$

Here we have introduced the notation

$$f(x) = \frac{3j_1(x)}{x}, \quad (18)$$

where  $j_1(x)$  is the spherical Bessel function of the first kind such that  $f(0) = 1$ . The second term in Eq. (14),  $G_{\text{osc}}$ , describes the quantum interference resulting from the scattering of the electrons by the defect

$$G_{\text{osc}}(r_0, d) = G_0(a_1)\Gamma(\mathbf{r}_0) + G_0(a_2)\Gamma(\mathbf{r}'_0) + 2G_{12}\Psi(\mathbf{r}_0, \mathbf{r}'_0)/f(k_F d), \quad (19)$$

where  $\mathbf{r}'_0 = (\rho_0 - \mathbf{d}, z_0)$ , and  $r'_0$  is the distance between the defect and the second contact. The functions  $\Gamma(\mathbf{r}_0)$  and  $\Gamma(\mathbf{r}'_0)$  account for interference of electron waves passing through the contact and returning to the same contact after scattering by the defect,

$$\Gamma(\mathbf{r}) = \frac{1}{F(z)} \sin \delta_0 \frac{z^2}{r^2} [12j_1(k_F r) \gamma(k_F r) + 6(1 - j_0(2k_F z)) \times (k_F r)^{-4} ((kr)^2 + 1) \sin \delta_0], \quad (20)$$

where

$$F(z) = 1 + 2 \sin \delta_0 \left[ \left( \frac{1}{2(2k_F z)^2} - j_0(2k_F z) \right) \sin \delta_0 - y_0(2k_F z) \cos \delta_0 \right], \quad (21)$$

and

$$\gamma(\mathbf{r}) = -y_1(k_F r) \cos \delta_0 + \sin \delta_0 [j_1(k_F r) (j_0(2k_F z) - 1) + y_0(2k_F z) y_1(k_F r)]. \quad (22)$$

In the last term in Eq. (19),  $\Psi(\mathbf{r}_0, \mathbf{r}'_0)$  describes the interference of electron waves that arrive at the other contact after scattering by the defect,

$$\Psi(\mathbf{r}, \mathbf{r}') = F^{-1} \sin \delta_0 \frac{z^2}{r r'} [j_1(k_F r') \gamma(\mathbf{r}) + j_1(k_F r) \gamma(\mathbf{r}') + \sin \delta_0 (j_0(k_F d) - j_0(k_F \sqrt{4z^2 + d^2})) \times (j_1(k_F r) j_1(k_F r') - y_1(k_F r) y_1(k_F r'))]. \quad (23)$$

For  $a_2=0$  (i.e., when we have just a single contact) Eq. (14) coincides with the expression for the conductance of a tunnel point contact obtained in Ref. 20. Figure 3 illustrates the dependence of the oscillatory part of the conductance (19) on the position of the defect in the plane  $z=z_0$ . The oscillatory pattern shown in Fig. 3 represents an image which could be obtained by DSTM when mapping the tunnelling conductance in the vicinity of a subsurface defect.

The general formula for the conductance (14) can be simplified for large distances between the contacts and

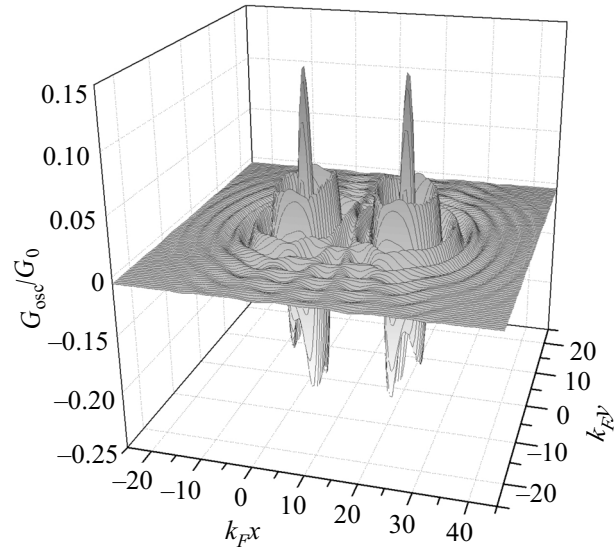


FIG. 3. The normalized oscillatory part of the conductance  $G_{\text{osc}}/G_0$  as a function of the defect position  $\rho_0$  in the  $z=0$  plane parallel to the interface;  $k_F z_0=5$ . The distance between the contacts is taken to be  $k_F d=20$ , and the scattering phase shift is  $\delta_0=1.5$ .

the defect,  $r_0, r'_0 \gg 1k_F$ , and for a weak scattering potential  $\delta_0 \approx -gm^* k_F / 2\pi\hbar^2 \ll 1$ . Under these assumptions, the normalized oscillatory part of the conductance can be written in a linear approximation in  $g$  as

$$\frac{G_{\text{osc}}}{G_0} = -6\delta_0 \frac{z_0^2}{k_F^2} \left\{ \frac{1}{r_0^4} \sin 2k_F r_0 + \frac{1}{r_0'^4} \sin 2k_F r_0' - \frac{2f(k_F d)}{(r_0 r_0')^2} \sin k_F (r_0 + r_0') \right\}. \quad (24)$$

For simplicity we take here  $a_1=a_2=a$ . Equation (24) shows that in contrast to one tunnel point contact, for which  $G_{\text{osc}} \sim \sin 2k_F r_0$  when  $k_F r_0 \gg 1$ , the oscillatory dependence of the double contact has a phase shift  $\vartheta$  that depends on the distance between the contacts

$$\frac{G_{\text{osc}}}{G_0} \sim \sin(2k_F r_0 + \vartheta), \quad (25)$$

where

$$\vartheta(\rho_0, z_0, d) = -\arcsin \left[ \frac{\sin 2\varphi + 2f(k_F d) \sin \varphi}{\sqrt{2 + 4f^2(k_F d) + 4f(k_F d) (\cos 2\varphi + 2 \cos \varphi)}} \right], \quad d \ll r_0, \quad (26)$$

and  $\Phi = k_F \rho_0 d / r_0$ . The defect position in the plane parallel to the surface,  $\rho_0$ , is known from the interference pattern of the conductance oscillations (see Fig. 3). In principle, the depth  $z_0$  of the defect can be found from the experimental data in the following way: changing the distance between the contacts over a small range  $\Delta d \ll d$  leads to the appearance of an additional phase shift  $\Delta \vartheta(\rho_0, z_0, d)$ , which can be determined

from the dependence  $G_{\text{osc}}(\rho_0, z_0, d)$ . (See Fig. 4.) The depth  $z_0$  can be found as a numerical solution of the equation

$$\Delta \vartheta = \vartheta'_d(\rho_0, z_0, d) \Delta d. \quad (27)$$

Let us now consider applying a magnetic field  $\mathbf{H}$  parallel to the surface of the sample (see Fig. 1). If the external magnetic field is sufficiently weak, such that the radius of the

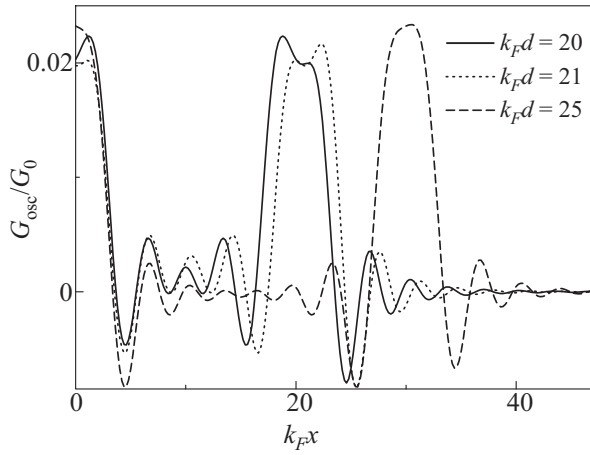


FIG. 4. Dependences of the oscillatory part of the conductance on the coordinate  $x_0$  of the defect for different distances between the contacts, with  $y_0=0$ ,  $k_F z_0=5$ , and  $\delta_0=0.1$ .

electron trajectories  $r_H = \hbar c k_F / eH$  is much greater than the distances between the positions of the contacts and the impurity,  $r_0, r'_0$ , the magnetic distortions of the trajectories<sup>21</sup> are negligible, i.e., the trajectories can be considered as straight lines.

Under this condition of  $r_H \gg r_0, r'_0$ , the zero-field wavefunction  $\psi(\mathbf{r})$  acquires an additional phase,

$$\tilde{\psi}(\mathbf{r}) = \psi(\mathbf{r}) \exp\left(\frac{ie}{c\hbar} \int_0^{\mathbf{r}} \mathbf{A}(\mathbf{r}'') d\mathbf{r}''\right), \quad (28)$$

and the Green function similarly takes the form<sup>16</sup>

$$\tilde{G}(\mathbf{r}, \mathbf{r}_0) = G(\mathbf{r}, \mathbf{r}_0) \exp\left(\frac{ie}{c\hbar} \int_{\mathbf{r}_0}^{\mathbf{r}} \mathbf{A}(\mathbf{r}'') d\mathbf{r}''\right). \quad (29)$$

Here,  $\mathbf{A}(\mathbf{r})$  is the vector potential of the magnetic field.

Because of this change in the wave function (28) the formula for the conductance  $G$  is modified, becoming

$$G = G_c(a_1, a_2) + \tilde{G}_{\text{osc}}(r_0, d, H), \quad (30)$$

$$\begin{aligned} \tilde{G}_{\text{osc}}(r_0, d, H) = & G_0(a_1) \Gamma(\mathbf{r}_0) + G_0(a_2) \Gamma(\mathbf{r}'_0) \\ & + 2G_{12} \tilde{\Psi}(\mathbf{r}_0, \mathbf{r}'_0) / f(k_F d), \end{aligned} \quad (31)$$

$$\begin{aligned} \tilde{\Psi}(\mathbf{r}, \mathbf{r}') = & \frac{1}{F} \sin \delta_0 \frac{z^2}{r'} \left[ j_1(k_F r') \left( \gamma(\mathbf{r}) \cos \frac{\pi\Phi}{\Phi_0} \right. \right. \\ & \left. \left. + \tilde{\gamma}(\mathbf{r}) \sin \frac{\pi\Phi}{\Phi_0} \right) + j_1(k_F r) \left( \gamma(\mathbf{r}') \cos \frac{\pi\Phi}{\Phi_0} \right. \right. \\ & \left. \left. + \tilde{\gamma}(\mathbf{r}') \sin \frac{\pi\Phi}{\Phi_0} \right) + \sin \delta_0 (j_0(k_F d) \right. \\ & \left. - j_0(k_F \sqrt{4z^2 + d^2}) \right) (j_1(k_F r) j_1(k_F r') \\ & \left. - y_1(k_F r) y_1(k_F r')) \right], \end{aligned} \quad (32)$$

$$\begin{aligned} \tilde{\gamma}(\mathbf{r}) = & \cos \delta_0 j_1(k_F r) + \sin \delta_0 \{ y_1(k_F r) (j_0(2k_F z) - 1) \\ & - y_0(2k_F z) j_1(k_F r) \}, \end{aligned} \quad (33)$$

where  $\gamma(\mathbf{r})$  is defined by Eq. (22),  $\Phi_0 = \pi c \hbar / e$  is the flux

quantum and  $\Phi = \mathbf{H}\mathbf{S}$  is the magnetic flux through the triangle formed by the vectors  $\mathbf{r}_0$  and  $\mathbf{r}'_0$  and the vector  $\mathbf{d}$  joining the contacts. For  $H=0$  Eq. (30) reduces to the formula (14) obtained earlier.

For  $r_0 \gg 1/k_F$  and  $\delta_0 \ll 1$ , Eq. (31) takes the form

$$\begin{aligned} \frac{\Delta G_{\text{osc}}(r_0, d, H)}{G_0} \approx & - \frac{12 \delta_0 z_0^2 f(k_F d)}{k_F^2 (r_0 r'_0)^2} \left[ \cos k_F r_0 \sin \left( k_F r'_0 \right. \right. \\ & \left. \left. - \frac{\pi\Phi}{\Phi_0} \right) + \cos k_F r'_0 \sin \left( k_F r_0 - \frac{\pi\Phi}{\Phi_0} \right) \right]. \end{aligned} \quad (34)$$

Similar oscillations in the electron local density of states have been predicted<sup>22</sup> for a system of two adatoms and an STM tip in a plane perpendicular to a surface magnetic field.

If the period of the oscillations is known, the depth  $z_0$  can be determined using the following procedure: in the most convenient geometry for the experiment the contacts should be placed so that the vectors  $\mathbf{r}_0, \mathbf{r}'_0$  and the normal to the sample surface lie in the same plane, i.e., the vectors  $\mathbf{H}$  and  $\mathbf{S}$  are parallel. For our illustration in Fig. 1 that means the coordinate  $\rho_0$  of the defect in the  $xy$  plane is on the line connecting the tips. In this case the relation between the period of oscillations  $\Delta H$  and the depth  $z_0$  is very simple:

$$z_0 = \frac{4\Phi_0}{d\Delta H}. \quad (35)$$

Note that observing the conductance oscillations (34) requires a sufficiently strong magnetic field. A magnetic field up to 15 T is currently attainable in low temperature STM.<sup>23</sup> For example, in order to record the period  $\Delta H$  for  $z_0 = d = 20$  nm it is necessary to apply a field of  $H = 5$  T. For typical metals, where  $\lambda_F \sim 0.1$  nm, for the given distance between the contacts and the defect  $r_0 \geq 10$  nm the amplitude of conductance oscillations becomes very small  $G_{\text{osc}} \sim G_0 (\lambda_F / r_0)^2 \sim (10^{-4} - 10^{-5}) G_0$ . Therefore more appropriate subjects for the proposed magnetic method of determining the position of subsurface defects include semiconductors and semimetals (Bi, Sb and their ordered alloys) where the Fermi wave length  $\lambda_F \sim 10$  nm. Also, a large amplitude  $G_{\text{osc}} \sim (10^{-2} - 10^{-3}) G_0$  could be expected in the metals of the first group, a Fermi surface of which has small cavities with effective mass  $m^* \approx (10^{-2} - 10^{-3}) m_0$  ( $m_0$  is the mass of a free electron). Low temperature STM could be used to avoid electron-phonon scattering along the electron trajectory.

In this paper we have investigated theoretically the conductance of a system consisting of two close tunnel point contacts with a point defect in their vicinity. The oscillatory dependence of the conductance on the separation between the contacts and their distances from the defect has been studied in the  $s$ -wave scattering approximation, which is valid for short range scattering potentials. We have proposed an alternative method for determining the depth of a subsurface impurity by measuring the phase change in the conductance oscillations which arise when the distance between the contacts of double-tip STM is varied. We have also found that, when there is a low magnetic field parallel to the surface of the sample, the depth of the subsurface impurity can be found easily from the period of Aharonov–Bohm oscillations in the conductance that develop in this case.

<sup>a</sup>Email: Kolesnichenko@ilt.kharkov.ua

- 
- <sup>1</sup>P. Jasninsky, P. Coenen, G. Pirug, and B. Voigtlander, *Rev. Sci. Instrum.* **77**, 093701 (2006).
- <sup>2</sup>H. Okamoto and D. Chen, *Rev. Sci. Instrum.* **72**, 4398 (2001).
- <sup>3</sup>W. Yi, I. I. Kaya, I. B. Altfeder, I. Appelbaum, D. M. Chen, and V. Narayanamurti, *Rev. Sci. Instrum.* **76**, 063711 (2005).
- <sup>4</sup>H. Grube, B. C. Harrison, J. Jia, and J. J. Boland, *Rev. Sci. Instrum.* **72**, 4388 (2001).
- <sup>5</sup>M. E. Flatte and J. M. Byers, *Phys. Rev. B* **53**, 10536(R) (1996).
- <sup>6</sup>P. Jaschinsky, J. Wensorra, M. I. Lepsa, J. Mysliveček, and B. Voigtlander, *J. Appl. Phys.* **104**, 094307 (2008).
- <sup>7</sup>J. M. Byers and M. E. Flatte, *Phys. Rev. Lett.* **74**, 306 (1995).
- <sup>8</sup>Q. Niu, M. C. Chang, and C. K. Shih, *Phys. Rev. B* **51**, 5502 (1995).
- <sup>9</sup>R. Dana, I. Kiruschev, P. D. Tran, P. Doppelt, and Y. Manassen, *Israel J. Chem.* **48**, 87 (2008).
- <sup>10</sup>Ye. S. Avotina, Yu. A. Kolesnichenko, and J. M. van Ruitenbeek, *Fiz. Nizk. Temp.* **36**, 1066 (2010) [*Low Temp. Phys.* **36**, 849 (2010)].
- <sup>11</sup>K. Kobayashi, *Phys. Rev. B* **54**, 17029 (1996).
- <sup>12</sup>Ye. S. Avotina, Yu. A. Kolesnichenko, A. N. Omelyanchouk, A. F. Otte, and J. M. van Ruitenbeek, *Phys. Rev. B* **71**, 115430 (2005).
- <sup>13</sup>Ye. S. Avotina, Yu. A. Kolesnichenko, A. F. Otte, and J. M. van Ruitenbeek, *Phys. Rev. B* **74**, 085411 (2006).
- <sup>14</sup>Ye. S. Avotina, Yu. A. Kolesnichenko, S. B. Roobol, and J. M. van Ruitenbeek, *Fiz. Nizk. Temp.* **34**, 268 (2008); , [*Low Temp. Phys.* **34**, 207 (2008)].
- <sup>15</sup>A. Wiesmann, M. Wenderoth, S. Lounis, P. Zahn, N. Quaas, R. G. Ulbrich, P. H. Dederichs, and S. Blugel, *Science* **323**, 1190 (2009).
- <sup>16</sup>A. Cano and I. Paul, *Phys. Rev. B* **80**, 153401 (2009).
- <sup>17</sup>I. O. Kulik, Yu. N. Mitsai, and A. N. Omelyanchouk, *Zh. Eksp. Theor. Phys. [Sov. Phys. JETP]* **63**, 1051 (1974).
- <sup>18</sup>E. Granot and M. Ya. Azbel, *Phys. Rev. B* **50**, 8868 (1994); , *J. Phys.: Condens. Matter* **11**, 4031 (1999).
- <sup>19</sup>A. A. Abrikosov, *Fundamentals of the Theory of Metals*, North Holland (1988).
- <sup>20</sup>Ye. S. Avotina, Yu. A. Kolesnichenko, and J. M. van Ruitenbeek, *J. Phys. Condens. Matter* **20**, 115208 (2008).
- <sup>21</sup>Ye. S. Avotina, Yu. A. Kolesnichenko, A. F. Otte, and J. M. van Ruitenbeek, *Phys. Rev. B* **75**, 125411 (2007).
- <sup>22</sup>A. Cano and I. Paul, *Phys. Rev. B* **80**, 153401 (2009).
- <sup>23</sup>V. Shvarts, Z. Zhao, L. Bobb, and M. Jirmanus, *J. Phys.: Conf. Ser.* **150**, 012046 (2009).

This article was published in English in the original Russian journal. Reproduced here with stylistic changes by AIP